International Journal of Engineering Research ISSN:2319-6890)(online),2347-5013(print)
Volume No.3 Issue No: Special 1, pp: 124-131 22nd March 2014

Bending Behaviour Of Exponentially Graded Material Plates Using New Higher Order Shear Deformation Theory with Stretching Effect

B. Sidda Reddy
School of Mechanical Engineering, R.G.M. College of Engineering & Technology, Nandyal, Kurnool (Dt), A.P, India-518501
Corresponding Email:bsrrgmcet@gmail.com

Abstract— **In the present paper, a new shear strain shape function is proposed to study the static analysis of exponentially graded material plates (EGMPs). This theory satisfies the zero transverse shear stress conditions on the top and bottom surface of the plates. The modulus of elasticity is assumed to vary exponentially through the thickness direction. The governing differential equations and boundary conditions are derived by employing the Hamilton's principle. Navier type closed form solutions are obtained for EGMPs subjected to bi-sinusoidal mechanical loads for simply supported boundary conditions. The accuracy of the present results is established by comparing those with 3-D elasticity solutions and with well known trigonometric shear deformation theory. From the present results, it can be concluded that the proposed theory is accurate and efficient in predicting the static bending behaviour of exponentially graded material plates..**

.Keywords— Exponentially graded material plates, static behaviour, Analytical solutions, Hamilton's principle.

I. Introduction

FGMs are widely used in many structural applications such as mechanics, civil engineering, optical, electronic, chemical, mechanical, biomedical, energy sources, nuclear, automotive fields and ship building industries to eliminate stress concentration and relax residual stresses and enhance bond strength. These materials also have great potential in applications where the operating conditions are severe, including spacecraft heat shields, heat exchanger tubes, fly wheels, plasma facings for fusion reactors, biomedical implants, engine components, and high power electrical contacts or even magnets. Different combinations of the ordinarily incompatible functions can be implemented to create new materials for chemical plants, aerospace, nuclear energy reactors, etc. For example, a discrete layer of ceramic material is bonded to a metallic structure in a conventional thermal barrier coating for high temperature environments. However, the abrupt transition in material properties across the interface between distinct materials can cause large inter-laminar stresses and lead to plastic deformation [1]. These damaging effects can be eased by grading the material constituents spatially. In high thermal environments, large concentrations of ceramic material are placed at corrosive and high temperature locations, while large concentrations of metal are placed in regions where mechanical properties are needed to be high.

Hence, to use them efficiently, a good understanding of their structural and dynamical behavior and also a precise knowledge of the deformation characteristics, stress distribution, natural frequencies and buckling loads under various load conditions are required. The computational modelling of FGM is an important tool for the understanding of the structural and dynamic behavior and also acquiring the knowledge on static, vibration and buckling responses of structures.

The literature on the FGPs is relatively scarce when compared to isotropic and laminated plates. In the past, researches on plates have received immense attention, and a variety of plate theories have been proposed to study the mechanical behavior of FGM plates. In particular, knowledge pertaining to static analysis, free vibration and buckling is essential for optimal design of structures. For example, our numerical results clearly show that, one could achieve an optimal design for FGM plates with a suitable power law index "*n*". It is useful to present some developments in the plate theory. The Classical plate theory (CPT) provides acceptable results only for the analysis of thin plates and neglects the transverse shear effects. However, for moderately thick plates CPT under predicts deflections and over predicts buckling loads and natural frequencies. The first-order shear deformation theories (FSDTs) are based on Reissner [2] and Mindlin [3] accounts for the transverse shear deformation effect by means of a linear variation of in-plane displacements and stresses through the thickness of the plate, but requires a correction factor to satisfy the free transverse shear stress conditions on the top and bottom surfaces of the plate. Although, the FSDT provides a sufficiently accurate description of response for thin to moderately thick plates, it is not convenient to use due to difficulty with determination of the correct value of shear correction factor. In-order to overcome the limitations of FSDT many HSDTs were developed that involve higher order terms in Taylors expansions of the displacements in the thickness coordinate. The finite element formulation of a higher-order shear deformation theory is presented by Kant et. al [4] which considers three dimensional Hooke's law, incorporates the effect of transverse normal strain in addition to transverse shear deformations.

Kant and Swaminathan [5] have developed analytical formulations and solutions to study the static analysis of simply supported composite and sandwich plates using higher order shear deformation theory. The developed model incorporates the laminate deformations that account for the effects of transverse shear deformation, transverse normal strain/stress and a nonlinear variation of in-plane displacements with respect to the thickness coordinate-thus eliminated the need of shear correction coefficients. Zenkour [6] presented the generalized shear deformation theory to study the static response is presented for a simply supported functionally graded rectangular plate subjected to a transverse uniform load. The effective material properties are estimated using simple power-law distribution in terms of the volume fractions of the Constituents. They also studied the influence of transversal shear deformation, plate aspect ratio, side-to-thickness ratio, and volume fraction distributions.

Ferreira et al. [7] have analyzed the static deformations of functionally graded plates using the collocation method, the radial basis functions and a higher-order shear deformation theory. They employed an optimization procedure based on the cross-validation technique to select the shape parameter in the radial basis functions and used the Mori-Tanaka homogenization technique to deduce effective properties of functionally graded materials.

Carrera et al. [8] employed the unified formulation and the principle of virtual displacements to obtain both closed-form and finite element solutions for the static analysis of functionally graded material plates subjected to transverse mechanical loadings. The unified formulation covers the order of the expansion ranges from 1 to 4, thus covers first-order as well as higher order.

Gilhooley et al. [9] has analyzed two-dimensional static and dynamic deformations of FGMs with material response modelled as either linear elastic or as linear viscoelastic using the meshless local Petrov–Galerkin method. They employed the multiquadric radial basis function to approximate the trial solution.

Shao and Ma [10] analyzed the functionally graded hollow circular cylinders subjected to thermo-mechanical loads and assumed that material properties are temperature independent and vary continuously in the radial direction of cylinder. They obtained the solutions for the time-dependent temperature and thermo-mechanical stresses by employing the Laplace transform techniques and series solving method for ordinary differential equation.

Mantari and Soares [11] presented an analytical solution to the static analysis of functionally graded plates (FGPs) by using a new trigonometric higher-order theory in which the stretching effect is included.

In the present paper, analytical formulations and solutions to the bending behaviour of exponentially graded material plates subjected to lateral pressure is developed using a new shear strain shape function considering thickness stretching. This theory accounts for adequate distribution of the transverse shear strains in the thickness of the plate and satisfies the traction free boundary conditions on the top and bottom surface of the plates, thus a shear correction factor is not required. The accuracy of the present results is established by comparing those with 3-D elasticity solutions and with well known trigonometric shear deformation theory.

II. Formulation of higher order theory

Consider a rectangular plate of length *a*, width *b* and thickness *h*, composed of functionally graded material through the thickness as shown in Fig. 1 with the adopted coordinate system. The material properties are assumed to be varied in the thickness direction only. On the top surface (z=+h/2), the plate is composed of full ceramic and graded to the bottom surface (z=-h/2) that composed of full metal. The reference surface is the middle surface of the plate (z=0). The functionally graded material plate properties are assumed to be the function of the volume fraction of constituent materials and vary exponentially through the thickness as indicated in:

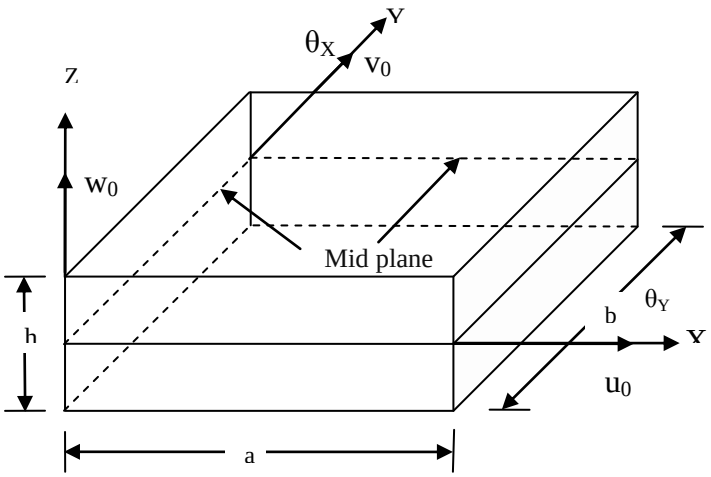

Fig 1: Functionally graded material plate with the adopted coordinate system

$$P(z) = e^{p\left(\frac{z}{h}+\frac{1}{2}\right)} P_b \quad \textbf{(1)}$$

Where P denotes the effective material property, P_b denotes the property on the bottom surface of the plate and *p* is the material variation parameter that dictates the material variation profile through the thickness and takes value greater than zero. On the top surface at z=+h/2, the plate is composed of full ceramic and graded to the bottom surface at z=-h/2, the composed of full metal. The effective material properties of the plate, including Young's modulus, E, density ρ, and shear modulus, G, vary according to Eq. (1), and poisons ratio (υ) is assumed to be constant.

Displacement Field:

In the present work, the following displacement field including thickness stretching effect and with new shear strain function for the first time is proposed.

$$u(x,y,z) = u_0(x,y) + z\left[\left(f^* + \frac{r}{h}\cos\left(\frac{rz}{h}\right)\right)\theta_x(x,y) + f^*\frac{\partial\theta_z}{\partial x} - \frac{\partial w_0}{\partial x}\right]$$

$$v(x,y,z) = v_0(x,y) + z\left[\left(f^* + \frac{r}{h}\cos\left(\frac{rz}{h}\right)\right)\theta_y(x,y) + f^*\frac{\partial\theta_z}{\partial y} - \frac{\partial w_0}{\partial y}\right]$$

$$w(x,y,z) = w_0(x,y) + \left[\frac{r}{h}\cos\left(\frac{rz}{h}\right) - z\frac{r^2}{h^2}\mathrm{Sin}\left(\frac{rz}{h}\right)\right]\theta_z(x,y) \quad (2)$$

Where $f^* = \dfrac{r^2\sin\left(\frac{r}{2}\right)}{2h} - \dfrac{r}{h}\cos\left(\frac{r}{2}\right)$

In the above relations, the parameters u_0, v_0 are the in plane displacements and w_o is the transverse displacement of a point (x, y) at the mid plane. The functions θ_x, θ_y and θ_z are shear deformations at the mid-plane. The coefficient of shear deformations are the shear strain shape functions and are selected in such a way that the present theory allows for realistic prediction of displacements and stress distribution across the thickness of the plate [12]. The above proposed displacement field automatically satisfies the zero transverse shear stress conditions on the top and bottom surface to the plates ($\tau_{xz,}\ \tau_{yz} = 0$ at z=±h/2).

The displacement function is a parameter "r" dependent and therefore needs to be selected or calculated. The optimal value of "r" is ascertained after several computations of the plate governing Eq. (8a-8f) to reach the shear stress $\tau_{xz}\,at\,(0, b/2, 0)$ which gives closest results to three dimensional elasticity solutions provided by Zenkour [13]. Details will be discussed after finding the plate governing differential equations.

Strain displacement relations:

The linear stain displacement relations associated with the proposed displacement field as given in Eq. (2a-d) under the assumption of small deformations, small rotations and obeys Hooke's law and valid for thin to thick plates under consideration are given as:

$$\varepsilon_{xx} = \varepsilon^0_{xx} + zk_{xx} + \frac{rz}{h}\cos\left(\frac{rz}{h}\right)k^*_{xx} \quad 3(a)$$

$$\varepsilon_{yy} = \varepsilon^0_{yy} + zk_{yy} + \frac{rz}{h}\cos\left(\frac{rz}{h}\right)k^*_{yy} \quad 3(b)$$

$$\varepsilon_{zz} = -\left(\frac{r^3 z}{h^3}\cos\left(\frac{rz}{h}\right) + \frac{2r^2}{h^2}\mathrm{Sin}\left(\frac{rz}{h}\right)\right)k^*_{zz} \quad 3(c)$$

$$\gamma_{xy} = \gamma^0_{xy} + zk_{xy} + \frac{rz}{h}cos\left(\frac{rz}{h}\right)k^*_{xy} \quad 3(d)$$

$$\gamma_{yz} = \gamma^0_{yz} + \left[\frac{r}{h}cos\left(\frac{rz}{h}\right) - z\frac{r^2}{h^2}Sin\left(\frac{rz}{h}\right)\right]k^*_{yz} \quad 3(e)$$

$$\gamma_{xz} = \gamma^0_{xz} + \left[\frac{r}{h}cos\left(\frac{rz}{h}\right) - z\frac{r^2}{h^2}Sin\left(\frac{rz}{h}\right)\right]k^*_{xz} \quad 3(f)$$

Where

$$\varepsilon^0_{xx} = \frac{\partial u_0}{\partial x}, \quad 4(a)$$

$$k_{xx} = f^*\left(\frac{\partial\theta_x}{\partial x} + \frac{\partial^2\theta_z}{\partial x^2}\right) - \frac{\partial^2 w_0}{\partial x^2}, \quad 4(b)$$

$$k^*_{xx} = \frac{\partial\theta_x}{\partial x} \quad 4(c)$$

$$\varepsilon^0_{yy} = \frac{\partial v_0}{\partial y}, \quad 4(d)$$

$$k_{yy} = f^*\left(\frac{\partial\theta_y}{\partial y} + \frac{\partial^2\theta_z}{\partial y^2}\right) - \frac{\partial^2 w_0}{\partial y^2}, \quad 4(e)$$

$$k^*_{yy} = \frac{\partial\theta_y}{\partial y} \quad 4(f)$$

$$k^*_{zz} = \theta_z \quad 4(g)$$

$$\gamma^0_{xy} = \frac{\partial u_0}{\partial y} + \frac{\partial v_0}{\partial y} \quad 4(h)$$

$$k_{xy} = f^*\left(\frac{\partial\theta_x}{\partial y} + \frac{\partial\theta_y}{\partial x} + 2\frac{\partial^2\theta_z}{\partial x\partial y}\right) - 2\frac{\partial^2 w_0}{\partial x\partial y} \quad 4(i)$$

$$k_{xy}^{*}=\frac{\partial\theta_x}{\partial y}+\frac{\partial\theta_y}{\partial x}$$

4(j)

$$\gamma_{yz}^{0}=f^{*}\left(\theta_y+\frac{\partial\theta_z}{\partial y}\right)$$

4(k)

$$k_{yz}^{*}=\theta_y+\frac{\partial\theta_z}{\partial y}$$

4(l)

$$\gamma_{xz}^{0}=f^{*}\left(\theta_x+\frac{\partial\theta_z}{\partial x}\right)$$

4(m)

$$k_{xz}^{*}=\theta_x+\frac{\partial\theta_z}{\partial x}$$

4(n)

2.2 Constitutive Relations

The constitutive relations depend on which assumption of ε_z consider. If $\varepsilon_z\neq 0$, i.e., thickness stretching is allowed then the 3D model is used. In the case of functionally graded materials the constitutive equations can be written as:

$$\begin{Bmatrix}\sigma_{xx}\\ \sigma_{yy}\\ \sigma_{zz}\\ \tau_{xy}\\ \tau_{yz}\\ \tau_{xz}\end{Bmatrix}=\begin{bmatrix}Q_{11}&Q_{12}&Q_{13}&0&0&0\\ Q_{12}&Q_{22}&Q_{23}&0&0&0\\ Q_{13}&Q_{23}&Q_{33}&0&0&0\\ 0&0&0&Q_{44}&0&0\\ 0&0&0&0&Q_{55}&0\\ 0&0&0&0&0&Q_{66}\end{bmatrix}\begin{Bmatrix}\varepsilon_{xx}\\ \varepsilon_{yy}\\ \varepsilon_{zz}\\ \gamma_{xy}\\ \gamma_{yz}\\ \gamma_{xz}\end{Bmatrix} \quad (5)$$

Where(σ_{xx}, σ_{yy}, σ_{zz}, τ_{xy}, τ_{yz}, τ_{xz})t are the stresses and (ε_{xx}, ε_{yy}, ε_{zz}, γ_{xy}, γ_{yz}, γ_{xz})^t are the strains with respect to the axes, Q_{ij}'s are the three-dimensional elastic coefficients in the plate axes that vary through the plate thickness, given by

$$Q_{11}=Q_{22}=Q_{33}=\frac{(1-\upsilon^2)E(z)}{1-3\upsilon^2-2\upsilon^3};$$

(6a)

$$Q_{12}=Q_{13}=Q_{23}=\frac{\upsilon(1+\upsilon)E(z)}{1-3\upsilon^2-2\upsilon^3};$$

(6b)

$$Q_{44}=Q_{55}=Q_{66}=\frac{E(z)}{2(1+\upsilon)};$$

(6c)

$$E(z)=e^{p\left(\frac{z}{h}+\frac{1}{2}\right)}E_b \quad (6d)$$

Where E_m is the modulus of elasticity of the metal.

Governing Equations of Motion

The governing equations of motion of present theory are derived using the Hamilton's principle can be written in the analytical form as:

$$\int_0^T(\delta U+\delta V)\,dt=0$$

(7)

Where δU is the virtual strain energy and δV is the virtual work done by applied forces and is given by:

$$\delta U=\int_A\left\{\int_{-h/2}^{h/2}\left[\sigma_{xx}\delta\varepsilon_{xx}+\sigma_{yy}\delta\varepsilon_{yy}+\sigma_{zz}\delta\varepsilon_{zz}+\tau_{xy}\delta\gamma_{xy}+\tau_{xz}\delta\gamma_{xz}+\tau_{yz}\delta\gamma_{yz}\right]dz\right\}dx\,dy$$

(7a)

$$\delta V=-\int q\,\overline{w}\,dx\,dy$$

(7b)

Substituting for δU and δV in the virtual work statement in Eq. (7) and integrating through the thickness, integrating by parts and collecting the coefficients of $\delta u_o,\delta v_o,\delta w_o,\delta\theta_x,\delta\theta_y,\delta\theta_z$ the following equations of motion are obtained.

$$\delta u_0:\frac{\partial N_1}{\partial x}+\frac{\partial Q_1}{\partial y}=0$$

8(a)

$$\delta v_0:\frac{\partial N_2}{\partial y}+\frac{\partial Q_1}{\partial x}=0$$

8(b)

$$\delta w_0:\frac{\partial^2 M_1}{\partial x^2}+\frac{\partial^2 M_2}{\partial y^2}+2\frac{\partial^2 R_1}{\partial x\partial y}+q=0$$

8(c)

$$\delta\theta_x:f^{*}\frac{\partial M_1}{\partial x}+f^{*}\frac{\partial R_1}{\partial y}+\frac{\partial P_1}{\partial x}+\frac{\partial S_1}{\partial y}+f^{*}Q_3+S_3=0$$

8(d)

$$\delta\theta_y:f^{*}\frac{\partial M_2}{\partial y}+f^{*}\frac{\partial R_1}{\partial x}+\frac{\partial P_1}{\partial y}+\frac{\partial S_1}{\partial x}+f^{*}Q_2+R_3=0$$

8(e)

$$\delta\theta_z:f^{*}\frac{\partial^2 M_1}{\partial x^2}+f^{*}\frac{\partial^2 M_2}{\partial y^2}-2f^{*}\frac{\partial^2 R_1}{\partial x\partial y}+f^{*}\frac{\partial Q_2}{\partial y}+f^{*}\frac{\partial Q_3}{\partial x}+\frac{\partial R_2}{\partial y}+\frac{\partial S_3}{\partial x}-f^{*}q-N_3=0$$

8(f)

The equations of motion (8) can be expressed in terms of displacements u_o, v_0, w_0, θ_x, θ_y θ_z and by substituting for the force and moment resultants. For homogenous exponentially graded plates, the equations of motion (8) in terms of displacements.

III. Analytical solutions for EGM plates

Rectangular plates are generally classified by referring to the type of support used. A closed form Navier type solution is implemented for simply supported exponentially graded material plates to ensure the accuracy of the proposed higher order theory which is free from computational/numerical error. Here concerned with the analytical solutions of the Eq. (8a) - (9k) for simply supported EG plates. Navier solution is derived for a rectangular plate with dimensions (a×b×h) and all edges of the plate are simply supported. Under these boundary conditions, the plate is subjected to the following boundary conditions.

At x=0, a,; $N_1= M_1= P_1= v_0= w_0= \theta_y= \theta_z=0$

At y=0, b; $N_2= M_2= P_2= u_0= w_0= \theta_x= \theta_z=0$

The sinusoidal variation of transverse load and temperature is considered as under:

$$q\ (x,y,t) = \sum_{m=1}^{\infty}\sum_{n=1}^{\infty} q_{mn}(t)\ \sin\alpha x\ \sin\beta y \tag{9}$$

Solution functions that completely satisfy the above boundary conditions in Eq. (10) are assumed as follows:

$$u_0\ (x,y) = \sum_{m=1}^{\infty}\sum_{n=1}^{\infty} U_{mn}\ \cos\alpha x\ \sin\beta y \quad , 0\le x\le a;\ 0\le x\le b; \tag{12a}$$

$$v_0\ (x,y,t) = \sum_{m=1}^{\infty}\sum_{n=1}^{\infty} V_{mn}\ \sin\alpha x\ \cos\beta y \quad 0\le x\le a;\ 0\le x\le b; \tag{12b}$$

$$w_0\ (x,y) = \sum_{m=1}^{\infty}\sum_{n=1}^{\infty} W_{mn}\ \sin\alpha x\ \sin\beta y \quad , 0\le x\le a;\ 0\le x\le b; \tag{12c}$$

$$\theta_x\ (x,y) = \sum_{m=1}^{\infty}\sum_{n=1}^{\infty} X_{mn}\ \cos\alpha x\ \sin\beta y \quad , 0\le x\le a;\ 0\le x\le b; \tag{12d}$$

$$\theta_y\ (x,y) = \sum_{m=1}^{\infty}\sum_{n=1}^{\infty} Y_{mn}\ \sin\alpha x\ \cos\beta y \quad , 0\le x\le a;\ 0\le x\le b; \tag{12e}$$

$$\theta_z\ (x,y) = \sum_{m=1}^{\infty}\sum_{n=1}^{\infty} Z_{mn}\ \sin\alpha x\ \sin\beta y \quad , 0\le x\le a;\ 0\le x\le b; \tag{12f}$$

Where

$\alpha = \frac{m\pi}{a}$ and $\beta = \frac{n\pi}{b}$ and m and n are modes numbers

Substituting the assumed solution of Eq. (10a) - (10f) in to governing differential equations given by Eq. (8a-8f), simplification of these equations lead to a set of 6 simultaneous equation involving six unknown amplitudes (U_{mn}, V_{mn}, W_{mn}, X_{mn}, Y_{mn}, Z_{mn}) which can be solved by any suitable numerical technique. These equations can be expressed in matrix form as

$[S]_{6\times6}[\Delta]_{6\times1}=[F]_{6\times1}$

Where [S] collects all stiffness terms and Δ are the unknown amplitudes and [F] is the force matrix.

IV. Results and Discussion

Numerical results of the present higher order shear deformation theory are presented for various aspect ratios (b/a) and different values of the exponent *p*. Poisson's ratio is assumed to be a constant, υ=0.3. Table 1-2 present results of centre plate deflections for various side to thick ratios, a/h = {2, 4} respectively. The present results are excellent agreement with the 3-D elasticity solutions and solutions provided by Mantari and Guedes Soares [11]. The present theory slightly under predicts the 3-D elasticity solutions for larger values of aspect ratios and slightly over predicts for smaller values of aspect ratios. Therefore, the importance of including the thickness stretching for accuracy and tendency is crucial. The nondimensionalized centre deflections decreases as exponent p increases, and also when b/a decrease.

Table 3 presents the transverse normal stress results for various aspect ratios and various powerlaw index values (p) at a/h=2. From the Table it is seen that the transverse stress increases with the increase of index value. Also, observed that the present results are close agreement with the 3-D elasticity solutions. Table 4 presents the axial stress results for various aspect ratios and various powerlaw index values (p) at a/h=10. From the Table it is seen that the axial stress also increases with the increase of index value. Also, observed that the present results are close agreement with the Mantari et al.[11] solutions.

The variation of nondimensionalized shear stress $\bar{\sigma}_{xz}(0,b/2,0)$ is presented in Table 5. From the Table it is seen that the transverse shear stresses decreases with the increase of exponent p and also with aspect ratio b/a.

V. Conclusions

A thickness stretching new trigonometric higher order shear deformation theory has been developed for the simply supported FGM plates to obtain displacements and stresses under mechanical loading.

The displacements and stresses predicted by the present theory were compared to 3-D elasticity solutions and other trigonometric shear deformation theory results published in the literature. The results considering $\varepsilon_z \neq 0$ showed very good agreement with the published results in the literature. Even for a thinner FGM plates the σ_z effects should always be considered in the formulation.

The variations of material properties across the thickness direction affect the displacements and stresses in FGM plates under mechanical loading

Table 1: compariosn of Non-dimensionalized center deflection for various exponentially graded rectangular plates, a/h=2

b/a	Theory	n=0.1	n=0.3	n=0.5	n=0.7	n=1	n=1.5
6	3-D[13]	1.63774	1.48846	1.35184	1.22688	1.05929	0.82606
	Present	**1.63511**	**1.47824**	**1.33528**	**1.20512**	**1.03168**	**0.79307**
	Mantari & Guedes[11]	1.63654	1.47953	1.33644	1.20618	1.03325	0.79387
5	3-D[13]	1.60646	1.46007	1.32607	1.20349	1.03907	0.81024
	Present	**1.60552**	**1.45148**	**1.31109**	**1.18327**	**1.01293**	**0.77858**
	Mantari & Guedes[11]	1.60532	1.4513	1.31094	1.18315	1.01352	0.77867
4	3-D[13]	1.55146	1.41013	1.28074	1.16235	1.00352	0.78241
	Present	**1.55335**	**1.4043**	**1.26844**	**1.14474**	**0.97987**	**0.75304**
	Mantari & Guedes[11]	1.55042	1.40166	1.2661	1.14267	0.97884	0.75195
3	3-D[13]	1.44295	1.3116	1.19129	1.08117	0.93337	0.7275
	Present	**1.44989**	**1.31074**	**1.18388**	**1.06835**	**0.91435**	**0.70243**
	Mantari & Guedes[11]	1.4421	1.30373	1.17761	1.06279	0.91041	0.69925
2	3-D[13]	1.19445	1.08593	0.9864	0.8952	0.77266	0.60174
	Present	**1.21032**	**1.094**	**0.9881**	**0.89153**	**0.76275**	**0.58546**
	Mantari & Guedes[11]	1.19408	1.07949	0.97503	0.8799	0.75377	0.57862
1	3-D[13]	0.57693	0.52473	0.47664	0.4324	0.37269	0.28904
	Present	**0.59653**	**0.53918**	**0.48681**	**0.43905**	**0.37528**	**0.28737**
	Mantari & Guedes[11]	0.57789	0.5224	0.47179	0.42567	0.36485	0.27939

Table 2: comparison of Non-dimensionalized center deflection for various exponentially graded rectangular plates, a/h=4

b/a	Theory	n=0.1	n=0.3	n=0.5	n=0.7	n=1	n=1.5
	3-D[13]	1.1714	1.06218	0.96331	0.87378	0.75501	0.59193
6	**Present**	**1.16886**	**1.05693**	**0.9551**	**0.86254**	**0.73943**	**0.57058**
	Mantari & Guedes[11]	1.17033	1.05825	0.95628	0.86359	0.74032	0.57128
5	3-D[13]	1.14589	1.03906	0.94236	0.85478	0.73859	0.57904
	Present	**1.14378**	**1.03425**	**0.9346**	**0.84402**	**0.72354**	**0.55829**
	Mantari & Guedes[11]	1.14484	1.0352	0.93545	0.84478	0.72419	0.55882
4	3-D[13]	1.10115	0.99852	0.9056	0.82145	0.70979	0.55643
	Present	**1.09976**	**0.99444**	**0.89862**	**0.81151**	**0.69565**	**0.53673**
	Mantari & Guedes[11]	1.10013	0.99477	0.89891	0.81178	0.69589	0.53696
3	3-D[13]	1.01338	0.91899	0.8335	0.75606	0.65329	0.51209
	Present	**1.01328**	**0.91624**	**0.82793**	**0.74765**	**0.64087**	**0.49438**
	Mantari & Guedes[11]	1.01243	0.91546	0.82724	0.74704	0.64037	0.49408
2	3-D[13]	0.81529	0.73946	0.67075	0.60846	0.52574	0.412
	Present	**0.81747**	**0.73916**	**0.66788**	**0.60308**	**0.51686**	**0.39854**
	Mantari & Guedes[11]	0.81448	0.73647	0.66547	0.60093	0.51508	0.39732
1	3-D[13]	0.349	0.31677	0.28747	0.26083	0.22534	0.18054
	Present	**0.35253**	**0.31873**	**0.28794**	**0.25993**	**0.22262**	**0.17139**
	Mantari & Guedes[11]	0.3486	0.31519	0.28477	0.2571	0.22028	0.16972

Table 3: Nondimensionaized normal stress $\bar{\sigma}_{yy}(a/2, b/2, h/2)$ for EG rectangular plates, a/h=2

b/a	Theory	n=0.1	n=0.3	n=0.5	n=0.7	n=1	n=1.5
6	3-D[13]	0.29429	0.31008	0.32699	0.34508	0.37456	0.43051
	Present	**0.287573**	**0.307863**	**0.329499**	**0.352583**	**0.390152**	**0.461525**
	Mantari & Guedes[11]	0.27628	0.29544	0.31592	0.3378	0.37374	0.44163
5	3-D[13]	0.29674	0.31277	0.32993	0.34829	0.37821	0.435
	Present	**0.289506**	**0.309965**	**0.33178**	**0.355049**	**0.392912**	**0.464812**
	Mantari & Guedes[11]	0.27892	0.29833	0.31905	0.34119	0.37755	0.44614
4	3-D[13]	0.30084	0.31727	0.33486	0.35368	0.38435	0.44257
	Present	**0.292721**	**0.313467**	**0.335582**	**0.359166**	**0.397525**	**0.470309**
	Mantari & Guedes[11]	0.28335	0.30317	0.32431	0.3469	0.38394	0.45373
3	3-D[13]	0.30808	0.32525	0.34362	0.36329	0.39534	0.45619
	Present	**0.298331**	**0.319595**	**0.342254**	**0.366405**	**0.405654**	**0.480019**
	Mantari & Guedes[11]	0.29122	0.31177	0.33369	0.35707	0.39537	0.46732
2	3-D[13]	0.31998	0.33849	0.35833	0.37956	0.41417	0.47989
	Present	**0.306894**	**0.329072**	**0.352684**	**0.377822**	**0.418605**	**0.495622**
	Mantari & Guedes[11]	0.30422	0.32613	0.34945	0.37427	0.41483	0.49052
1	3-D[13]	0.31032	0.32923	0.34953	0.37127	0.40675	0.47405
	Present	**0.288065**	**0.309891**	**0.333079**	**0.357696**	**0.39745**	**0.471842**
	Mantari & Guedes11[]	0.29244	0.31468	0.33826	0.36325	0.40405	0.47848

Table 4: Nondimensionalized normal stresses $\bar{\sigma}_{xx}(a/2, b/2, h/2)$ for EG rectangular plates, a/h=10.

b/a	theory	n=0.1	n=0.3	n=0.5	n=0.7	n=1.0	n=1.5	n=2.0	n=2.5	n=3.0
6	**Present**	**0.62302**	**0.6663**	**0.7122**	**0.76086**	**0.8394**	**0.9868**	**1.1576**	**1.3556**	**1.5851**
	Mantari et al.[11]	0.6014	0.6426	0.6864	0.7329	0.8084	0.951	1.1177	1.3124	1.9394
5	**Present**	**0.61089**	**0.6533**	**0.6983**	**0.74599**	**0.823**	**0.9675**	**1.135**	**1.3293**	**1.5543**
	Mantari et al.[11]	0.5895	0.6299	0.6727	0.7184	0.7923	0.9321	1.0955	1.2865	1.5091
4	**Present**	**0.58959**	**0.6305**	**0.6739**	**0.71987**	**0.7942**	**0.9336**	**1.0953**	**1.2829**	**1.5003**
	Mantari et al.[11]	0.5686	0.6075	0.6488	0.6928	0.7641	0.8989	1.0566	1.241	1.456
3	**Present**	**0.54761**	**0.5855**	**0.6257**	**0.66841**	**0.7373**	**0.8668**	**1.017**	**1.1915**	**1.3938**
	Mantari et al.[11]	0.5275	0.5635	0.6018	0.6425	0.7085	0.8335	0.98	1.1514	1.3514
2	**Present**	**0.45185**	**0.483**	**0.516**	**0.55108**	**0.6078**	**0.7145**	**0.8386**	**0.9831**	**1.1509**
	Mantari et al.[11]	0.434	0.4634	0.4947	0.528	0.5822	0.6849	0.8056	0.9473	1.113
1	**Present**	**0.21727**	**0.2319**	**0.2475**	**0.26412**	**0.2911**	**0.3422**	**0.4022**	**0.4727**	**0.5553**
	Mantari et al.[11]	0.2063	0.2199	0.2344	0.2499	0.2753	0.324	0.3819	0.4506	0.5317

Table 5: Non-dimensionalized shear stress $\bar{\sigma}_{xz}(0, b/2, 0)$ for EG rectangular plates, a/h=10.

b/a	Theory	n=0.1	n=0.3	n=0.5	n=0.7	n=1.0	n=1.5	n=2.0	n=2.5	n=3.0
6	Present	0.47521	0.47443	0.4729	0.4706	0.4657	0.4539	0.4379	0.4183	0.3955
	Mantari et al.[11]	0.4634	0.4626	0.461	0.4586	0.4536	0.4416	0.4253	0.4065	0.3845
5	Present	0.4696	0.4689	0.4673	0.465	0.4602	0.4486	0.4328	0.4134	0.3909
	Mantari et al.[11]	0.4579	0.4571	0.4556	0.4532	0.4483	0.4364	0.4203	0.4017	0.38
4	Present	0.4597	0.4589	0.4574	0.4552	0.4504	0.4391	0.4236	0.4046	0.3826
	Mantari et al.[11]	0.4482	0.4475	0.4459	0.4436	0.4388	0.4271	0.4114	0.3933	0.372
3	Present	0.4396	0.4388	0.4374	0.4352	0.4307	0.4198	0.4051	0.3869	0.3658
	Mantari et al.[11]	0.4286	0.4279	0.4264	0.4242	0.4196	0.4084	0.3934	0.3761	0.3558
2	Present	0.3907	0.3901	0.3888	0.3869	0.3828	0.3732	0.36	0.3439	0.3252
	Mantari et al.[11]	0.381	0.3803	0.379	0.377	0.373	0.363	0.3497	0.3344	0.3165
1	Present	0.2441	0.2437	0.2429	0.2417	0.2392	0.2332	0.2249	0.2148	0.2031
	Mantari et al.[11]	0.238	0.2376	0.2368	0.2356	0.233	0.2268	0.2185	0.2094	0.1985

References

i. M. Finot, S. Suresh. Small and large deformation of thick and thin-film multilayers: effect of layer geometry, plasticity and compositional gradients. J Mech Phys Solids, Vo. 44, 1996, pp.683–721.

ii. E.Reissner, ASME. The effect of transverse shear deformation on the bending of elastic plates, Journal of Applied Mechanics, Vol. 12, No. 2, 1945, pp.69-77.

iii. RD. Mindlin. Influence of rotary inertia and shear on flexural motions of isotropic, elastic plates. Journal of Applied Mechanics, Vol. 18, 1951, pp.31-38.

iv. R. D. x mKant, , DRJ.Owen, OC Zienkiewicz, A refined higher order C^0 plate element, Computers and structures, Vol. 15, No. 2, 1988, pp.177-183.

v. T. Kant, and K Swaminathan. Analytical solutions for the static analysis of laminated composite and sandwich plates based on higher order refined theory. Composite structures, Vol. 56, No. 4,2002, pp.329-344.

vi. A.M. Zenkour. Generalized shear deformation theory for bending analysis of functionally graded plates. Applied mathematical modelling, Vol. 30, No. 1, 2006, pp.67-84.

vii. A. J. M. Ferreira, C. M. C. Roque, R. M. N. Jorge, G. E. Fasshauer, R. C. Batra. Analysis of Functionally Graded Plates by a Robust Meshless Method, Mechanics of Advanced Materials and Structures, Vol. 14, 2007, pp.577–587.

viii. E Carrera, S Brischetto, Robaldo. A Variable kinematic model for the analysis of functionally graded material plates, AIAA J, Vol. 46, 2008, pp.194-203.

ix. D.F. Gilhooley , J.R. Xiao , R.C. Batra , M.A. McCarthy J.W. Gillespie Jr. Two-dimensional stress analysis of functionally graded solids using the MLPG method with radial basis functions, Computational Materials Science, Vol. 41, 2008, pp.467–481.

x. Z.S. Shao, G.W. Ma. Thermo-mechanical stresses in functionally graded circular hollow cylinder with linearly increasing boundary temperature, Composite Structures, Vol. 83, 2008, pp.259–265.

xi. J.L. Mantari, C. Guedes Soares. A novel higher-order shear deformation theory with stretching effect for functionally graded plates, Composites: Part B, Vol. 45, 2013, pp.268–281.

xii. Neeraj Grover, D.K. Maiti and B.N. Singh, A new inverse hyperbolic shear deformation theory for static and buckling analysis of laminated composite and sandwich plates. Composite structures 95,2013, 667-675.

xiii. Zenkour AM. Benchmark trigonometric and 3-D elasticity solutions for an exponentially graded thick rectangular plate. Appl Math Model 2007;77:197-214.